Cell cycle-dependent cues regulate temporal patterning of the *Drosophila* central brain neural stem cells

Gonzalo N. Morales Chaya[1,2], Mubarak Hussain Syed[1]

[1]*Neural Diversity Lab, Department of Biology, University of New Mexico, Albuquerque, NM 87131, USA*
[2]*Institute of Neuroscience, Howard Hughes Medical Institute, University of Oregon, Eugene,OR 97403, USA*

contact: FlyGuy@unm.edu

Abstract

During nervous system development, diverse types of neurons and glia are sequentially generated by self-renewing neural stem cells (NSCs). Temporal changes in gene expression within NSCs are thought to regulate neural diversity; however, the mechanisms regulating the timing of these temporal gene transitions remain poorly understood. Drosophila type 2 NSCs, like human outer radial glia, divide to self-renew and generate intermediate neural progenitors, amplifying and diversifying the population of neurons innervating the central complex, a brain region crucial for sensorimotor coordination. Type 2 NSCs express over a dozen genes temporally, broadly classified as early and late-expressed genes. A conserved gene, seven-up, mediates early to late gene expression by activating ecdysone receptor (EcR) expression. However, the timing of EcR expression and, consequently, the transition from early to late gene expression remains unknown. This study investigates whether intrinsic mechanisms of cell cycle progression and cytokinesis are required to induce the NSC early-late transition. By generating mutant clones that arrest the NSC cell cycle or block cytokinesis, we show that both processes are necessary for the early-to-late transition. When NSCs are cell cycle or cytokinesis arrested, the early gene Imp fails to be downregulated and persists in the old NSCs, while the late factors EcR and Syncrip fail to be expressed. Furthermore, we demonstrate that the early factor Seven-up is insufficient to drive the transition, despite its normal expression in cell cycle- or cytokinesis-inhibited NSCs. These results suggest that both cell-intrinsic (cell cycle/cytokinesis) and extrinsic (hormone) cues are required for the early-late NSC gene expression transition.

Introduction

From insects to humans, multipotent neural stem cells (NSCs) generate diverse neurons and glia, which mediate proper nervous system function. Both spatial and temporal patterning programs regulate the diversity of neurons generated during nervous system development (Doe, 2017; El-Danaf et al., 2023; Enriquez et al., 2015; Erclik et al., 2017; Hamid et al., 2023; Kohwi and Doe, 2013; Malin and Desplan, 2021; Oberst et al., 2019; Sen, 2023; Skeath and Thor, 2003; Wani et al., 2023). While much is known about the regulation of spatial identity, the mechanisms underlying temporal identity are not entirely understood. Elucidating the processes through which NSCs undergo temporal patterning, enabling them to produce diverse neurons and glial cells in the nervous system, is critical for understanding brain development and disease. Studies on the Drosophila nervous system have identified temporal identity genes that express temporally in NSCs and diversify neural cell types (Bayraktar and Doe, 2013; Eldred et al., 2018; Isshiki et al., 2001; Li et al., 2013; Maurange et al., 2008; Syed et al., 2017; Yang et al., 2015; Chaya et al., 2025). Sim-

ilar temporal identity programs were later shown to regulate vertebrate retinal and cortical cell type specification (Alsiö et al., 2013; Elliott et al., 2008; Javed et al., 2023; Kohwi and Doe, 2013; Koo et al., 2023; Pebworth et al., 2021; Telley et al., 2019). In Drosophila embryonic NSCs, these gene transitions were thought to be intrinsically regulated; however, our recent findings in larval central brain NSCs identified the role of extrinsic steroid growth hormone ecdysone in the early-to-late gene transition (Syed et al., 2017). Recently, thyroid hormone signaling has been identified as regulating the early-to-late born cone cell type in human retinal organoid cultures (Eldred et al., 2018). Over the past few years, various temporally expressed genes have been identified in both invertebrates and vertebrates; however, the factors that determine the precise timing of these gene transitions are poorly understood.

Based on division patterns, the Drosophila NSCs can be classified as type 0, type 1, or type 2 NSCs. Type 0 NSCs generate a single post-mitotic neuron with each division and have only been observed in embryonic stages (Arefin et al., 2020; Baumgardt et al., 2014). Type 1 NSCs generate a ganglion mother cell (GMC) with each division; each GMC makes two post-mitotic neurons (Doe, 2017; Doe and Goodman, 1985; Rossi and Desplan, 2017). While type 1 NSCs comprise the majority of NSCs in the brain, type 2 NSCs—though limited to just 16—generate more complex and diverse progeny by exhibiting a more complex division pattern, producing approximately 5,000 neurons of at least about 160 distinct cell types (Epiney et al., 2025). Type 2 NSCs divide to self-renew and generate Intermediate Neural Progenitors (INPs); each INP undergoes a series of 4-6 self-renewing divisions to produce 4-6 GMCs, which each generate two neurons (Bello et al., 2008; Boone and Doe, 2008; Bowman et al., 2008; Wang et al., 2014). Recent temporal RNA-sequencing experiments have revealed that type 2 NSCs undergo a gene expression cascade involving transcription factors (TFs) and RNA-binding proteins (RBPs). In early larvae 0-60h after larval hatching (ALH), the NSCs express TFs, Seven-up (Svp), Castor (Cas), Chinmo, and RBPs, IGF-II mRNA-binding protein (Imp), and Lin-28. In late larvae (60-120h ALH), the NSCs express TFs, Ecdysone receptor (EcR), Ecdysone-induced protein 93F (E93), Broad and RBP, Syncrip (Syp) (Ren et al., 2017; Syed et al., 2017). The early-expressed conserved transcription factor Svp regulates the expression of EcR, thereby rendering NSCs competent to respond to the extrinsic hormonal signal, which triggers the early-late gene expression switch (Syed et al., 2017). While the role of the extrinsic factor Ecdysone in triggering the early-late transition is understood, nothing is known about how intrinsic factors drive this transition and what regulates the timing of these events.

In vertebrate cortical development, the cell cycle plays a key role in regulating a neural progenitor's ability to respond to extrinsic cues. Transplanted progenitors in a late-stage host exhibit different responses to these cues depending on their cell cycle stage at the time of transplantation (McConnell and Kaznowski, 1991; Ohnuma and Harris, 2003). In Drosophila, several studies have demonstrated a relationship between the cell cycle and temporal gene expression programs in NSCs. Interestingly, this relationship differs markedly between embryonic and larval stages. In embryonic NSCs, the classic temporal cascade—Hunchback > Kruppel > Pdm1/2 > Castor—is largely cell-intrinsic and can proceed in isolated, G2-arrested cells (Grosskortenhaus et al., 2005). While the transition from Hunchback to Kruppel requires cytokinesis, subsequent transitions (Kruppel to Pdm1/2 to Castor) occur even when cell cycle progression and cytokinesis are blocked.

In contrast, larval NSCs exhibit temporal transitions from early factors (Imp/Chinmo) to late factors (Syp/Broad) that depend on the cell's metabolic state and progression through the G1/S phase of the cell cycle (van den Ameele and Brand, 2019). Notably, at the end of larval neurogenesis, late temporal programs schedule the end of neurogenesis, and NSCs undergo cell cycle exit or apoptosis. These late-stage transitions are governed by the Svp-mediated induction of the EcR and its downstream effector E93 (Pahl et al., 2019; Homem et al., 2014; Maurange et al., 2008; Syed et al., 2017). However, whether Svp and EcR expression—and thus the timing of early-to-late transitions—are dependent on cell cycle progression remains unknown. Furthermore, it is not yet clear whether similar temporal and cell cycle interactions occur in type 1 and type 2 NSCs. Moreover, it is unclear whether the timing of NSC gene expression is driven by organismal cues (e.g., hormones or signaling pathways), internal cues (e.g., a cell cycle counting clock), or both. Here, we utilize larval central brain NSCs to investigate whether cell cycle and cytokinesis regulate the timing of

the temporal gene expression program.

Results

Cell cycle and cytokinesis are both required for the early-late temporal factor switch in type 2 NSCs

Our previous work revealed that in type 2 NSCs, the transition from early to late temporal factors occurs around 55h ALH (Syed et al., 2017). To better understand the mechanisms regulating the precise timing of these gene expression shifts, we next focused on the roles of the cell cycle and cytokinesis. While the cell cycle has been shown to influence temporal patterning in some systems, it appears to be dispensable in others, suggesting context-dependent roles in regulating these transitions (van den Ameele and Brand, 2019; Grosskortenhaus et al., 2005; Syed et al., 2017; Ray and Li, 2022). To investigate whether the temporal progression of type 2 NSCs requires cell cycle progression, we blocked the NSC cell cycle or cytokinesis in all type 2 NSCs using the driver Wor-GAL4, Ase-GAL80, starting at 0h ALH (the experimental model is shown in (**Figure 1**). We inhibited the cell cycle in all type 2 NSCs by knocking down Cyclin-dependent kinase 1 (Cdk1), a cdc2 kinase that forms heterodimers with Cyclin A and Cyclin B and is required for the execution of mitosis. Larvae were collected at 0 h ALH, and temporal factor expression was assayed at 72 h ALH. The Cdk1RNAi effectively blocked the cell cycle, as we could not observe any GFP-labeled progeny near the NSCs, and the NSC cell volume was larger than that of the control, which has also been attributed to normal cell-cycle progression (Hartenstein et al., 1987)(**Figure S1**). While all control type 2 NSC lineages showed normal temporal factor expression progression, Cdk1RNAi type 2 NSCs exhibited prolonged expression of the early factor Imp into later stages of development, and

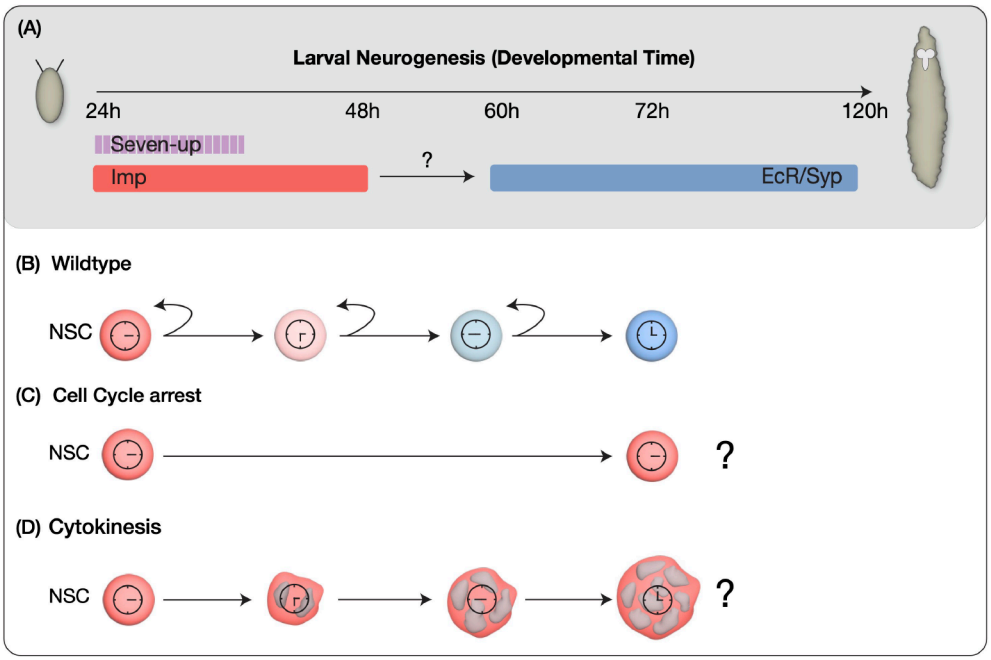

Figure 1: Models for early-to-late temporal progression transition of type 2 NSCs.
(A) Depicts timing of NSC temporal factor expression in type 2 NSCs during Drosophila larval development (B) Wild type NSCs undergo normal early to late temporal factor progression (C) Cell cycle progression as a regulator to allow timely expression of factors in NSCs (D) Cytokinesis dependent regulation of temporal gene expression.

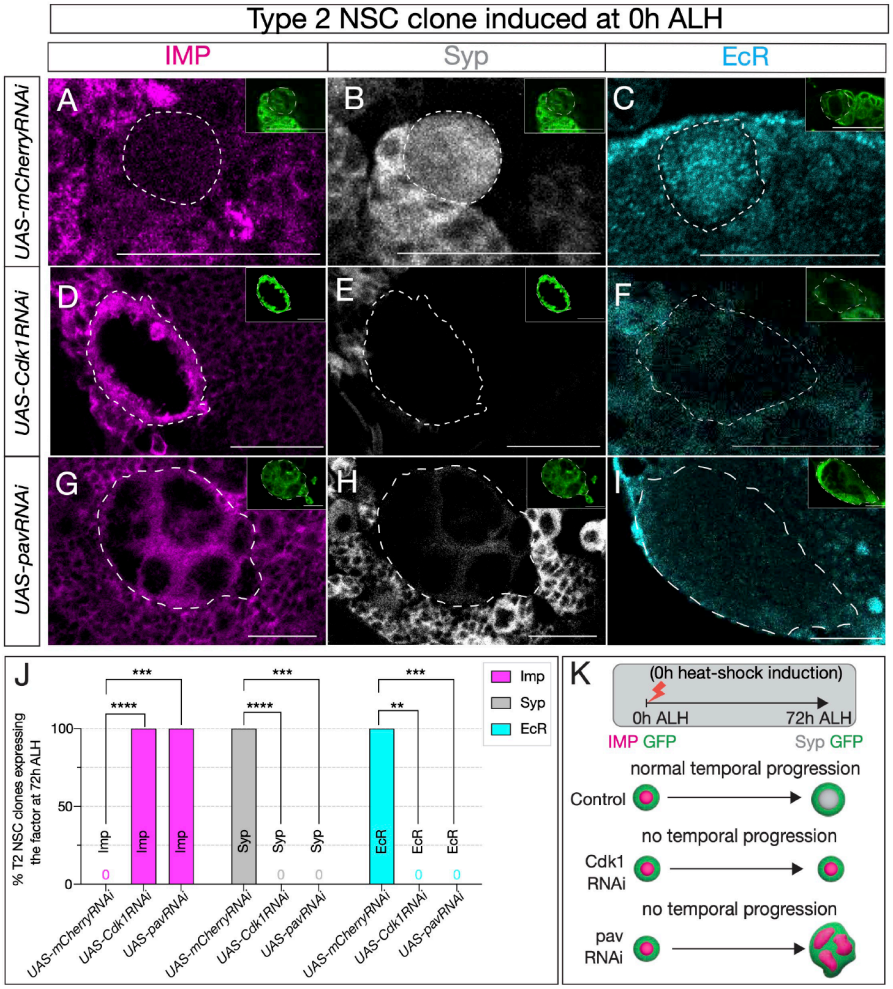

Figure 2: Cell cycle and cytokinesis are required for temporal gene expression progression in type 2 NSCs. (A-C) Type 2 NSC control mCherryRNAi clones (circled) at 72h ALH show normal temporal gene expression progression. Early factor Imp is off, and late factors Syp and EcR are on at 72h ALH (D-F) Cdk1RNAi type 2 NSC clone fail to down-regulate early factor Imp, and late factors Syp and EcR are not turned on. (G-I) Similarly, cytokinesis-blocked type 2 NSC clones using pavRNAi fail to down-regulate Imp and upregulate Syp and EcR. (J) Quantification of early (Imp) and late (EcR, Syp) temporal factor expression in mCherryRNAi, Cdk1RNAi, and pavRNAi type 2 NSCs (n ≥ 4 clones per genotype). Statistical analysis by Fisher's exact test: Imp: 0/5 vs 11/11 clones in Cdk1RNAi ($p = 0.0002$), 0/5 vs 8/8 in pavRNAi ($p = 0.0008$); EcR: 6/6 vs 0/4 in Cdk1RNAi ($p = 0.0048$), 6/6 vs 0/7 in pavRNAi ($p = 0.0006$); Syp: 5/5 vs 0/11 in Cdk1RNAi ($p = 0.0002$), 5/5 vs 0/8 in pavRNAi ($p = 0.0008$). Only one clone was found per animal. (K) Representation of experimental layout for inducing clones at 0h ALH and analysis at 72h ALH. Type 2 NSCs are identified as Asense-negative large cells expressing UAS-mcd8::GFP (green insets). Scale bars represent 20um.

failed to upregulate the late factors Syp and EcR (**Figure S2**), confirming that cell cycle is essential for the early-to-late gene transition.

To further ensure the cell-specificity of this phenotype, better quantify and allow NSCs to develop in an otherwise wild-type brain, we used the flip-out approach that induced random single cell clones of type 2 NSCs. We induced random clones by giving a heat shock at 0h ALH using the genotype hsflp, 10xUAS-mCD8GFP; Act>FRT-stop-FRT>-GAL4. Both control RNAi (UAS-mCherryRNAi) and experimental (UAS-Cdk1RNAi) clones were labeled by GFP, and type 2 hits were confirmed by lack of the type 1 Asense marker (Figure S1 E-G). After heat shock, we assayed the clones in 72h ALH larvae. In the control type 2 NSCs, as anticipated at 72h ALH, minimal or no expression of the early factor Imp was observed, alongside high expression of late factors EcR and Syp (Figure 2A-2C; quantified in Figure 2J). In contrast, the experimental type 2 NSCs, where the cell cycle was blocked, exhibited persistent expression of the early factor Imp and no expression of late factors EcR and Syp at 72h ALH (Figure 2D-2F; quantified in Figure 2J), thus confirming that cell cycle progression is indispensable for the early-late switch in temporal factor gene expression.

The failure to switch from early to late factors could arise from blocking the cell-cycle progression (as part of a gene expression "clock" or "timer") or from preventing cytokinesis, resulting in a daughter cell that may deliver feedback signals or partition transcriptional regulators out of the NSC. To discern between these possibilities, we inhibited cytokinesis, halting NSC progeny production while leaving its cell-cycle unaffected by expressing pavarotti RNAi (UAS-pavRNAi), a well-established cytokinesis inhibitor whose knockdown produces large, multinucleated cells (Grosskortenhaus et al., 2005; Adams et al., 1998). Similar to our previous observations (**Figure S2**), control type 2 NSCs showed no Imp expression and normal EcR/Syp expression (**Figure 2A-2C; quantified in 2J**), while the experimental pavRNAi type

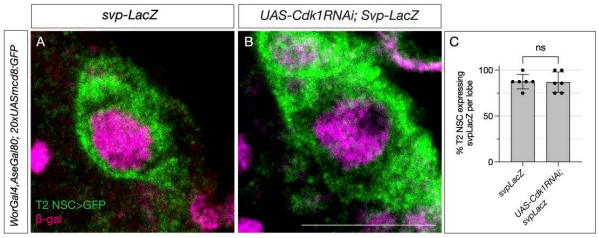

Figure 3: Switching factor Svp is expressed normally in cell-cycle-arrested type 2 NSCs. (A) Control type 2 NSCs marked in green show Svp-LacZ expression at 48h ALH. (B) Cell-cycle-arrested (Cdk1RNAi) type 2 NSCs express Svp-LacZ similar to the control (C) Quantification of LacZ expression in control and cell cycle blocked type 2 NSCs, n=6 for each genotype. Unpaired t-test, p-value = 0.9168. Scale bars represent 10um.

2 NSCs resulted in large multi-nucleated NSCs (**Figure S1 C-C'**) that maintained Imp expression and lacked EcR/Syp expression (**Figure 2 G-2I; quantified in 2J**). These results were consistent with blocking cytokinesis simultaneously in all type 2 NSCs (**Figure S2**). We conclude from these experiments that both, cell-cycle progression and cytokinesis are essential for the early-late gene expression switch in type 2 NSCs (**Figure 2K**).

The switching factor Svp is normally expressed in cell-cycle arrested NSCs

A conserved nuclear hormone receptor, Svp, mediates the early-to-late gene switch by regulating EcR expression (Dillon et al., 2024, Maurange et al., 2008, Syed et al., 2017). The svp mutant type 2 NSCs stay in their early gene expression module and fail to exit the cell cycle at the end of larval life. The mutant type 2 NSCs fail to downregulate the expression of early factors Chinmo and Imp and show no expression of the late factors EcR, Broad, Syncrip, and E93. While Svp shows its peak expression at 18-24h ALH, EcR expression starts at around 55h ALH (Dillon et al., 2024, Ren et al. 2017, Syed et al., 2017). Although svp is required for EcR expression, what regulates the precise timing of EcR expression around 55h ALH is unknown. The lack of EcR expression in cell cycle-arrested Type 2 NSCs could be due to either defective Svp ex-

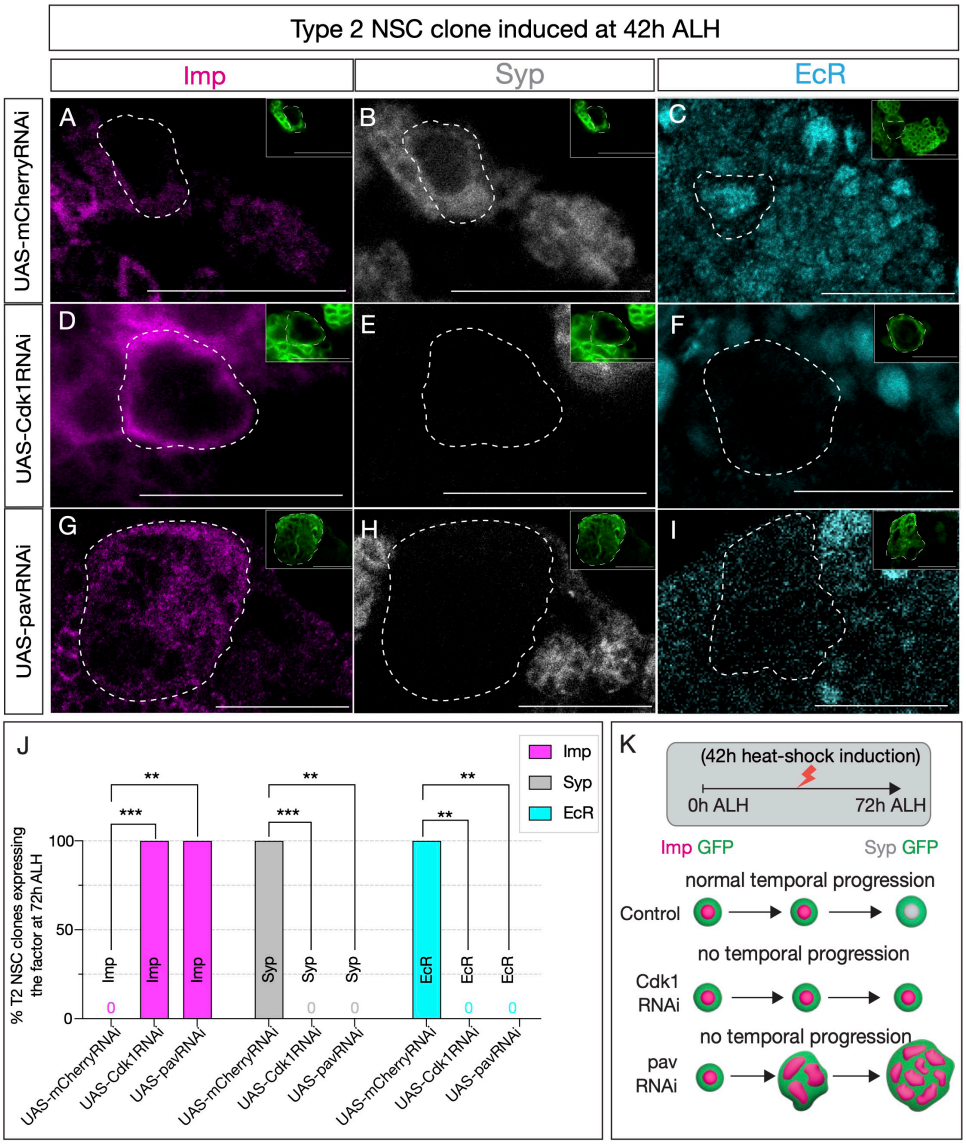

Figure 4: Early Svp expression is not sufficient to drive temporal factor progression in type 2 NSCs. (A-C)(A-C) Type 2 NSC control mCherryRNAi clones (circled) induced at 42h ALH and stained at 72h ALH show normal progression of temporal factors. Early factor Imp is off, and late factors Syp and EcR are on. (D-F) Cdk1RNAi clones show consistent failure to down-regulate early factor Imp and activate Syp and EcR (G-I) Likewise, pavRNAi clones fail to express EcR and Syp and consistently express early factor Imp. (J) Quantification of early (Imp) and late (EcR, Syp) temporal factor expression in control (UAS-mCherryRNAi), UAS-Cdk1RNAi, and UAS-pavRNAi type 2 NSCs (n ≥ 4 clones per geno-type). Statistical analysis by Fisher's exact test: Imp: Cdk1RNAi vs control p = 0.0002, pavRNAi vs control p = 0.0079; EcR: Cdk1RNAi vs control p = 0.0079, pavRNAi vs control p = 0.0079; Syp: Cdk1RNAi vs control p = 0.0002, pavRNAi vs control p = 0.0079. Only one clone was found per animal. (K) Representation of experimental layout. Clones are identified as Asense negative large cells expressing UAS-mcd8::GFP (green insets). Scale bars represent 20um.

pression or the lack of a cell cycle counter or both.

To test whether cell-cycle-arrested NSCs fail to express Svp and thus produce a phenotype similar to the svp mutant, we assayed Svp expression in type 2 cell-cycle-arrested NSCs. Since Svp expression is transient in these NSCs, we used a svpLacZ line, similar to our previous work (Syed et al., 2017), to achieve more stable protein expression. Upon counting LacZ-positive type 2 NSCs at 48h ALH, nearly all control type 2 NSCs showed svpLacZ expression (**Figure 3A**), and cell-cycle-arrested animals displayed similar expression levels with no statistically significant difference from controls (**Figure 3B, quantified in 3C**). We conclude that the timing of Svp expression is normal in cell-cycle-arrested NSCs.

Svp and cell cycle progression are independently required for the early-late temporal factor switch

Since Svp expression was normal in cell-cycle arrested type 2 NSCs, we wondered whether the cell cycle acts as a timer for the precise EcR expression following Svp expression. To address this question, we generated type 2 NSC clones expressing either Cdk1RNAi or pavRNAi at 42h ALH (see methods) well after the Svp expression window (18-24h ALH). We assayed for expression of NSC temporal markers at 72h ALH. If the transition fails to occur, it will confirm that Svp primes EcR expression, but the intrinsic cell cycle clock determines the precise timing. Conversely, if the transition occurs normally, cell cycle/cytokinesis plays a role in early gene expression (before 42h), but not in later, post-Svp expression. Compared to control type 2 NSC clones that showed normal Imp downregulation and EcR/Syp expression at 72h ALH (**Figure 4A-4C; quantified in 4J**), Cdk1 and pav mutant type 2 NSC clones had persistent Imp expression and no EcR/Syp expression (Figure 4D,4I; quantified in 4J), confirming that cell cycle progression post-Svp expression is critical for precise timing of EcR and early to late gene transition (Figure 3K).

Cell cycle and cytokinesis are required for the early-late temporal factor switch in type 1 NSCs

So far, we have focused on type 2 NSCs, which are relatively few; however, the majority of larval NSCs are type 1 NSCs, which express the same early and late temporal factors as type 2 NSCs (Syed et al., 2017). The timing of EcR expression and the transition from early to late gene expression also matches the type 2 NSC pattern (Syed et al., 2017). Thus, we sought to determine if cell cycle and cytokinesis also regulate temporal gene transitions in type 1 NSCs.

Similar to our previous experiments, we generated clones using the genotype hsFLP, UAS-mCD8GFP; Act>FRT-stop-FRT>GAL4 / UAS-Cdk1RNAi or UAS-mCherryRNAi and assayed GFP and Asense positive type 1 NSCs (**Figure S1. E'-G'**). Control RNAi induced at 0h and assayed at 72h showed normal down-regulation of Imp and expression of the late factors Syp (**Figure 5A-C and 5K-M; quantified in 5J and 5T**). In contrast, Cdk1 or pavRNAi type 1 NSC clones induced at 0h and assayed at 72h maintained Imp expression and lacked EcR/Syp expression (**Figure 5D-I; quantified in 5J**).

Similarly, Cdk1 or pavRNAi induced at 42h -- after the Svp expression window -- and assayed at 72h also maintained Imp expression and lacked EcR/Syp expression (**Figure 5N-S; quantified in 5T**). This suggests that most central brain NSCs possess a cell-cycle and cytokinesis-dependent, cell-intrinsic mechanism that regulates the Imp/Syp expression transition. Our studies indicate that all central brain NSCs require cell cycle and cytokinesis, together with the switching factor Svp expression, to drive the early-late temporal factor expression transition.

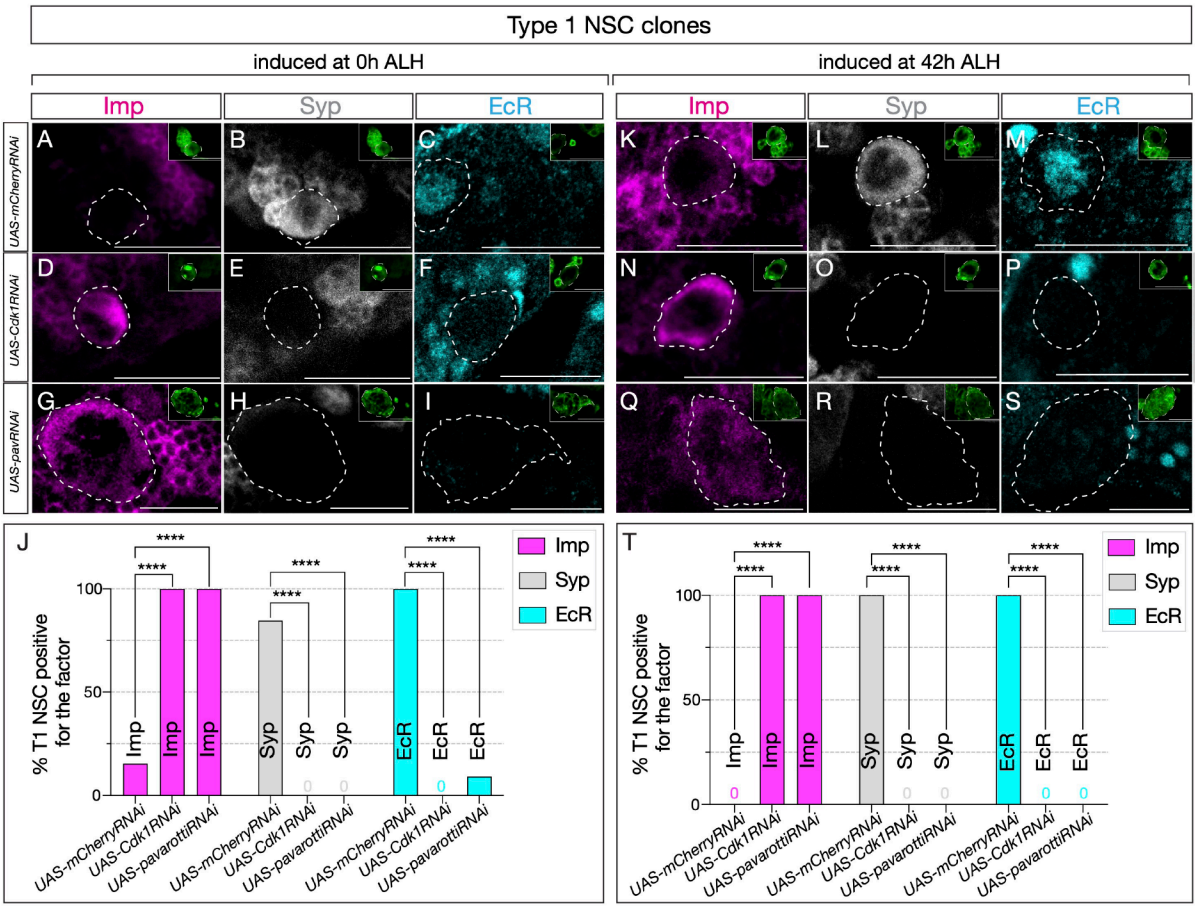

Figure 5: Cell cycle and cytokinesis are required for temporal progression in type 1 NSCs. (A-I). Clones were induced at 0h ALH, and for (K-S), clones were induced at 42h ALH. (A-C) Typ. (A-I). Clones were induced at 0h ALH, and for (K-S), clones were induced at 42h ALH. (A-C) Type 1 NSC control RNAi clones show normal expression of temporal factor progression. (D-F) Cell cycle blocked type 1 NSC clones using Cdk1RNAi show failure to up-regulate EcR and Syp, and consistent expression of early factor Imp. (G-I) pavRNAi type I NSC clones fail to downregulate early factor Imp, and late factors Syp and EcR fail to express. (K-M) Control type 1 NSC clones induced at 42h ALH show normal expression of early and late factors, while Cdk1RNAi clones (N-P) and pavRNAi clones (Q-S) fail to downregulate Imp and fail to activate late factors Syp and EcR. (J, T) Quantification of early and late factor expression of 0h and 42h ALH–induced clones. (J) In clones induced at 0h ALH, Imp was expressed in 10/10 Cdk1RNAi clones (2/13 control, p = 0.000067) and 12/12 pavRNAi clones (2/13 control, p = 0.000020). EcR was not detected in Cdk1RNAi (0/11) or pavRNAi clones (0/11), while it was expressed in 12/12 control clones (p = 0.000001 for both). Syp was absent in Cdk1RNAi (0/10) and pavRNAi clones (0/12), while present in 11/13 control clones (p = 0.000067 and p = 0.000020, respectively). (T) In clones induced at 42h ALH, Imp expression persisted in 10/10 Cdk1RNAi (0/10 control, p = 0.000011) and 13/13 pavRNAi clones (0/10 control, p = 0.000001). EcR expression was not detected in Cdk1RNAi (0/8) or pavRNAi clones (0/13), compared to 10/10 control (p = 0.000023 and p = 0.000001). Syp expression was not detected in Cdk1RNAi (0/10) or pavRNAi clones (0/13), but was regular in 10/10 control (p = 0.000011 and p = 0.000001). Only one clone was found per animal. For each genotype n≥8. Type 1 clones are identified as Asense-positive, large cells expressing mcd8::GFP (green insets). Scale bars represent 20um..

Discussion

Temporal patterning plays a crucial role in specifying the diverse cell types of the nervous system. While many temporally expressed genes have been identified in both Drosophila and vertebrate neural progenitors (Javed et al., 2023; Koo et al., 2023; Pebworth et al., 2021; Syed et al., 2017; Telley et al., 2019; Walsh and Doe, 2017), what governs the timing of these gene expression transitions is not clearly understood. Is there an intrinsic timer within NSCs that counts and regulates the precise timing of temporal gene transitions? Is such a mechanism linked to cell-cycle progression and cytokinesis? How are NSC intrinsic and extrinsic environmental cues coupled? This study investigated the cell-intrinsic mechanisms regulating the early-to-late temporal gene expression transitions. Using Drosophila larval central brain NSCs, we identified that both cell cycle and cytokinesis-dependent cell-intrinsic timers regulate the progression of gene expression. In cytokinesis-blocked NSCs, the transition from early Imp expression to late EcR and Syp expression was impeded in both type 1 and type 2 NSCs. Upon temporal cell cycle block at 42h ALH, we showed that normal cell cycle progression is still essential for EcR expression despite the Svp expression being normal in the NSCs. These findings provide insights into the possible mechanisms regulating the temporal gene transition timing and also reveal the complex interplay of the cell cycle, cell-intrinsic genes, and cell-extrinsic hormonal cues in determining the precise timing of neuron type production within neural progenitors.

The possible role of cell cycle and cytokinesis in regulating temporal patterning and neuronal identity has been studied in vertebrates and invertebrates (Doe, 2008; Grosskortenhaus et al., 2005; Hagey et al., 2020; Kawaguchi, 2019; van den Ameele J, Brand AH. 2019). In vertebrates, the G2/M phase is required for the sequential generation of layer-specific cortical neurons. Knockdown of G2/M regulators has been shown to prevent radial glial cells from maintaining a "young," multipotent state, leading to premature differentiation and a bias toward the production of early-born neurons (Hagey et al., 2020; Kawaguchi, 2019). In the case of Drosophila embryonic NSCs, which sequentially express Hunchback, Kruppel, Pdm1, and Castor, cell cycle is dispensable for these transitions. The initial Hunchback to Kruppel expression requires cytokinesis, while the Kruppel to Pdm1 to Castor transition occurs normally in G2 arrested NSCs (Grosskortenhaus et al., 2005). In contrast, our studies on larval NSCs show that both cell cycle and cytokinesis are essential for the early Imp/Chinmo to late EcR/Syncrip gene transition. The temporal gene progressions of embryonic NSCs occur normally in isolated NSCs, suggesting that these gene transitions are regulated intrinsically. In contrast, larval NSCs express EcR and require extrinsic growth hormone, ecdysone, for the transition from early to late gene expression. Our findings suggest that NSCs with more complex division patterns and dividing in situations where the growth and division patterns need to be coordinated require both cell-intrinsic and extrinsic cues. Studies on larval optic lobe NSCs thus far suggest that their temporal gene expression cascade is regulated cell-intrinsically, akin to embryonic NSCs (Konstantinides et al., 2022; Li et al., 2013). However, it remains unclear whether these temporal transitions depend on progression through the cell cycle/cytokinesis or both. This raises the intriguing question of whether optic lobe NSCs follow an embryonic-like model, in which temporal patterning occurs independently of cell division, or resemble larval central brain NSCs, where temporal progression is tightly coupled to the cell cycle and cytokinesis

Through the cell cycle, neural progenitors generate neurons populating distinct layers in the vertebrate cortex (Borrell and Calegari, 2014; Hagey et al., 2020; Ohtsuka and Kageyama, 2019; Salomoni and Calegari, 2010); however, the relationship between cell cycle and temporal patterning has remained elusive. Given that the cell cycle is essential for temporal gene transitions, it could be one potential way of timing the generation of distinct

progeny with precise temporal control. While we were able to demonstrate the cell-intrinsic roles of cell cycle in timing temporal gene transitions, given the fact that NSC resides in a glial niche and in close proximity to its lineages (Doe, 2008), and the cell-cycle blocked lineages have few or not progeny, we cannot not rule out the possibility that type 2 NSCs with cell cycle arrest failed to undergo normal temporal progression indirectly due to a lack of feedback signaling from their progeny. Additionally, we note that in some large multinucleated pavRNAi clones, a weak EcR signal can sometimes be observed near the cell membrane or within cytoplasmic regions (**Fig. 2I**). However, the nuclear compartments of these polynucleated cells—where EcR is normally localized and active—show no detectable EcR staining. The origin of this membrane-proximal EcR signal remains unclear; it may reflect non-specific antibody binding, altered EcR trafficking or degradation in cytokinesis-defective cells, or imaging artefacts arising from the large and irregular morphology of these clones. Importantly, the absence of nuclear EcR in the scored NSCs supports our conclusion that both cell cycle progression and cytokinesis are required for the acquisition of nuclear EcR expression and for the early-to-late temporal transition.

We acknowledge that we cannot formally exclude gene-specific, cell-cycle–independent roles of Cdk1 or Pav. However, several lines of evidence favor the interpretation that disruption of cell-cycle progression or cytokinesis underlies the phenotype. First, Cdk1 and Pav are canonical regulators of mitosis and cytokinesis, respectively; second, the same qualitative temporal-block phenotype (persistence of early markers and failure to induce late markers) is produced by orthogonal manipulations that prolong G1/S or slow proliferation, including G1/S inhibitors and mitochondrial OxPhos inhibition (which increases G1/S occupancy), reported by others (van den Ameele and Brand, 2019). Thus, although we cannot rule out additional, gene-specific contributions of Cdk1 or Pav, the concordant effects of multiple, mechanistically distinct cell-cycle perturbations make altered cell-cycle dynamics the most parsimonious explanation. Definitive understanding of the molecular mechanism (for example, whether mitosis-dependent chromatin remodeling, partitioning of factors during cytokinesis, or cell-cycle–regulated signaling triggers late-factor induction) will require further experiments.

Our results suggest that only part of the temporal gene cascade depends on cell-cycle progression. Depletion of Cdk1 disrupts the induction of late temporal factors (Syp, EcR) while leaving the onset of early switching factor Svp intact, indicating that the early expression of the temporal transition switching program can proceed independently of cell-cycle progression. This distinction raises specific mechanistic possibilities: for example, mitosis- or cytokinesis-coupled processes such as transcriptional reactivation, cell-cycle–dependent post-translational modification of regulators, or daughter-cell–mediated signaling/partitioning could be required for late-factor induction but not for early svp activation. Defining the precise mechanism is beyond the scope of this study; however, our findings provide a testable framework for future experiments to determine how cell-cycle–regulated changes in nuclear or cytoplasmic state enable the transition from early Imp/Chinmo to late Syp/EcR expression.

During cortical development, both cell cycle and extrinsic factors govern neuronal fate, and it was proposed that neuronal progenitors undergo cyclic changes in their ability to respond to extrinsic cues (McConnell and Kaznowski, 1991; Okamoto et al., 2016). Similarly, in Drosophila, Delta expression in the neighboring GMC and glia regulate Notch signaling, which is required for terminating neurogenesis in the central brain (Sood et al., 2024). Further studies are needed to elucidate the mechanism by which the cell cycle influences EcR expression and to confirm the role of progeny within the lineage in regulating temporal gene expression transitions in NSCs.

Acknowledgments

We thank Adil Wani, Asif Bakshi, Sen-Lin Lai, and Chris Doe for providing feedback on the manuscript. Thanks to Claude Desplan for sharing antibodies generously. Stocks obtained from the Bloomington Drosophila Stock Center (NIH P40OD018537) were used in this study. We thank UNM CETI Biology Cell Biology Core for providing a confocal microscope facility. The research was supported by the Sloan Research Fellowship FG-2023-20617, 2023 BBRF Young Investigator Grant, McKnight Scholars Award, National Science Foundation CAREER Award IOS-2047020, Air Force Office of Scientific Research FA9550-24-1-0214 and NINDS R01NS136555 to MHS

Author contributions

Conceptualization: G.M.C and M.H.S.; methodology: G.M.C.; visualization: G.M.C. and M.H.S.; writing-original draft: G.M.C.; editing: M.H.S.; funding acquisition: M.H.S. and supervision: M.H.S.

Competing interests

The authors declare no competing interest

Materials and Methods

Immunohistochemistry

Larval brains were dissected in PBS and mounted on poly-D-lysine-coated coverslips. Samples were fixed for 23 minutes in 4% PFA in PBST, and then washed in PBST for 3x20 minutes. Following, the samples were blocked with 2% normal donkey serum and 2% normal goat serum (Jackson ImmunoResearch Laboratories, Inc.) in PBST for 40 minutes at room temperature. Samples were then incubated in a primary antibody mix diluted in PBST overnight or for 1-2 days at 4°C. Primary antibodies were removed, and samples were thoroughly washed with PBST. Samples were then incubated in secondary antibodies for 2 hours at room temperature. Secondary antibodies were removed, and samples were washed in PBST. Samples were dehydrated with an ethanol series of 30%, 50%, 75%, and 100% ethanol, then incubated in xylene (Fisher Chemical X5-1) for 2x10 minutes. Samples were mounted onto slides with DPX (Sigma-Aldrich 06552) and cured for 3-4 days, then stored at 4°C until imaged.

Image acquisition and analysis

Fluorescent images were acquired on both Zeiss LSM 710 and 800. Scale bars were given for all stacks within maximum intensity projection images. Brightness and contrast were adjusted in the figure images individually for better visualization across the entire image in control and experimental samples. Statistics and bar graphs were computed using Prism 10.

Figure Preparation

Confocal images were prepared using FIJI or Imaris 10.0.0. Figures and schematics were assembled using Adobe Illustrator (2025).

Generation of clones

To generate RNAi clones, hsFLP;10xUASmcd8::GFP; ActFRTstopFRTGAL4 flies were crossed to the RNAi lines for the gene of interest or control UAS-mCherryRNAi line. Embryos were collected over a period of 4 hr. After hatching, larvae were collected and then heat shocked in a 37°C water bath for 8 minutes and reared at 25°C until the desired time point. Temporal factor expression (Imp, Syp, EcR) was scored as positive or negative in individual neuroblasts. Because pavRNAi clones are frequently large and often multinucleated, reliable nuclear segmentation and per-nucleus intensity quantification were not feasible. To ensure reproducibility across samples, we normalized fluorescence signal intensity for each neuroblast to the mean intensity of neighboring wild type neuroblasts imaged in the same field. A neuroblast was considered positive when

its normalized intensity in the nucleus was at least 2× the local background. This scoring criterion was applied uniformly to all genotypes and time points. Only one clone was quantified per animal unless otherwise indicated.

References

Adams RR, Tavares AAM, Salzberg A, Bellen HJ, Glover DM. 1998. pavarotti encodes a kinesin-like protein required to organize the central spindle and contractile ring for cytokinesis. Genes Dev 12:1483–1494. doi:10.1101/gad.12.10.1483

Alsiö JM, Tarchini B, Cayouette M, Livesey FJ. 2013. Ikaros promotes early-born neuronal fates in the cerebral cortex. Proc Natl Acad Sci U S A 110:E716-725. doi:10.1073/pnas.1215707110

Arefin B, Bahrampour S, Monedero Cobeta I, Curt JR, Stratmann J, Yaghmaeian Salmani B, Baumgardt M, Benito-Sipos J, Thor S. 2020. Development of the Drosophila melanogaster embryonic CNSPatterning and Cell Type Specification in the Developing CNS and PNS. Elsevier. pp. 617–642. doi:10.1016/B978-0-12-814405-3.00025-4

Baumgardt M, Karlsson D, Salmani BY, Bivik C, MacDonald RB, Gunnar E, Thor S. 2014. Global Programmed Switch in Neural Daughter Cell Proliferation Mode Triggered by a Temporal Gene Cascade. Dev Cell 30:192–208. doi:10.1016/j.devcel.2014.06.021

Bayraktar OA, Doe CQ. 2013. Combinatorial temporal patterning in progenitors expands neural diversity. Nature 498:449–455. doi:10.1038/nature12266

Bello BC, Izergina N, Caussinus E, Reichert H. 2008. Amplification of neural stem cell proliferation by intermediate progenitor cells in Drosophila brain development. Neural Develop 3:5. doi:10.1186/1749-8104-3-5

Boone JQ, Doe CQ. 2008. Identification of Drosophila type II neuroblast lineages containing transit amplifying ganglion mother cells. Dev Neurobiol 68:1185–1195. doi:10.1002/dneu.20648

Borrell V, Calegari F. 2014. Mechanisms of brain evolution: Regulation of neural progenitor cell diversity and cell cycle length. Neurosci Res 86:14–24. doi:10.1016/j.neures.2014.04.004

Bowman SK, Rolland V, Betschinger J, Kinsey KA, Emery G, Knoblich JA. 2008. The Tumor Suppressors Brat and Numb Regulate Transit-Amplifying Neuroblast Lineages in Drosophila. Dev Cell 14:535–546. doi:10.1016/j.devcel.2008.03.004

Chaya GNM, Hamid A, Wani AR, Gutierrez A, Syed MH. 2025. Developmental Genetic and Molecular Analysis of Drosophila Central Complex Lineages. Cold Spring Harb Protoc 2025:pdb.top108429. doi:10.1101/pdb.top108429

Dillon NR, Manning L, Hirono K, Doe CQ. 2024. Seven-up acts in neuroblasts to specify adult central complex neuron identity and initiate neuroblast decommissioning. Development 151:dev202504. doi:10.1242/dev.202504

Doe CQ, Goodman CS. 1985. Early events in insect neurogenesis. Dev Biol 111:206–219. doi:10.1016/0012-1606(85)90446-4

Doe CQ. 2008. Neural stem cells: balancing self-renewal with differentiation. Development 135:1575–1587. doi:10.1242/dev.014977

Doe CQ. 2017. Temporal Patterning in the Drosophila CNS. Annu Rev Cell Dev Biol 33:219–240. doi:10.1146/annurev-cellbio-111315-125210

El-Danaf RN, Rajesh R, Desplan C. 2023. Temporal regulation of neural diversity in Drosophila and vertebrates. Semin Cell Dev Biol 142:13–22. doi:10.1016/j.semcdb.2022.05.011

Eldred KC, Hadyniak SE, Hussey KA, Brenerman B, Zhang P-W, Chamling X, Sluch VM, Welsbie DS, Hattar S, Taylor J, Wahlin K, Zack DJ, Johnston RJ. 2018. Thyroid hormone signaling specifies cone subtypes in human retinal organoids. Science 362:eaau6348. doi:10.1126/science.aau6348

Elliott J, Jolicoeur C, Ramamurthy V, Cayouette M. 2008. Ikaros Confers Early Temporal Competence to Mouse Retinal Progenitor Cells. Neuron 60:26–39. doi:10.1016/j.neuron.2008.08.008

Enriquez J, Rio LQ, Blazeski R, Bellemin S, Godement P, Mason C, Mann RS. 2018. Differing Strat-

egies Despite Shared Lineages of Motor Neurons and Glia to Achieve Robust Development of an Adult Neuropil in Drosophila. Neuron 97:538-554.e5. doi:10.1016/j.neuron.2018.01.007

Enriquez J, Venkatasubramanian L, Baek M, Peterson M, Aghayeva U, Mann RS. 2015. Specification of Individual Adult Motor Neuron Morphologies by Combinatorial Transcription Factor Codes. Neuron 86:955–970. doi:10.1016/j.neuron.2015.04.011

Epiney D, Chaya GNM, Dillon NR, Lai S-L, Doe CQ. 2025. Transcriptional complexity in the insect central complex: single nuclei RNA-sequencing of adult brain neurons derived from type 2 neuroblasts. doi:10.7554/eLife.105896.2

Erclik T, Li X, Courgeon M, Bertet C, Chen Z, Baumert R, Ng J, Koo C, Arain U, Behnia R, Del Valle Rodriguez A, Senderowicz L, Negre N, White KP, Desplan C. 2017. Integration of temporal and spatial patterning generates neural diversity. Nature 541:365–370. doi:10.1038/nature20794

Grosskortenhaus R, Pearson BJ, Marusich A, Doe CQ. 2005. Regulation of Temporal Identity Transitions in Drosophila Neuroblasts. Dev Cell 8:193–202. doi:10.1016/j.devcel.2004.11.019

Hagey DW, Topcic D, Kee N, Reynaud F, Bergsland M, Perlmann T, Muhr J. 2020. CYCLIN-B1/2 and -D1 act in opposition to coordinate cortical progenitor self-renewal and lineage commitment. Nat Commun 11:2898. doi:10.1038/s41467-020-16597-8

Hamid A, Gutierrez A, Munroe J, Syed MH. 2023. The Drivers of Diversity: Integrated genetic and hormonal cues regulate neural diversity. Semin Cell Dev Biol 142:23–35. doi:10.1016/j.semcdb.2022.07.007

Hartenstein V, Rudloff E, Campos -Ortega JA. 1987. The pattern of proliferation of the neuroblasts in the wild-type embryo of Drosophila melanogaster. Rouxs Arch Dev Biol 196:473–485. doi:10.1007/BF00399871

Homem CCF, Steinmann V, Burkard TR, Jais A, Esterbauer H, Knoblich JA. 2014. Ecdysone and Mediator Change Energy Metabolism to Terminate Proliferation in Drosophila Neural Stem Cells. Cell 158:874–888. doi:10.1016/j.cell.2014.06.024

Isshiki T, Pearson B, Holbrook S, Doe CQ. 2001. Drosophila Neuroblasts Sequentially Express Transcription Factors which Specify the Temporal Identity of Their Neuronal Progeny. Cell 106:511–521. doi:10.1016/S0092-8674(01)00465-2

Javed A, Santos-França PL, Mattar P, Cui A, Kassem F, Cayouette M. 2023. Ikaros family proteins redundantly regulate temporal patterning in the developing mouse retina. Development 150:dev200436. doi:10.1242/dev.200436

Kawaguchi A. 2019. Temporal patterning of neocortical progenitor cells: How do they know the right time? Neurosci Res 138:3–11. doi:10.1016/j.neures.2018.09.004

Kohwi M, Doe CQ. 2013. Temporal fate specification and neural progenitor competence during development. Nat Rev Neurosci 14:823–838. doi:10.1038/nrn3618

Konstantinides N, Holguera I, Rossi AM, Escobar A, Dudragne L, Chen Y-C, Tran TN, Martínez Jaimes AM, Özel MN, Simon F, Shao Z, Tsankova NM, Fullard JF, Walldorf U, Roussos P, Desplan C. 2022. A complete temporal transcription factor series in the fly visual system. Nature 604:316–322. doi:10.1038/s41586-022-04564-w

Koo B, Lee K-H, Ming G, Yoon K-J, Song H. 2023. Setting the clock of neural progenitor cells during mammalian corticogenesis. Semin Cell Dev Biol 142:43–53. doi:10.1016/j.semcdb.2022.05.013

Li X, Erclik T, Bertet C, Chen Z, Voutev R, Venkatesh S, Morante J, Celik A, Desplan C. 2013. Temporal patterning of Drosophila medulla neuroblasts controls neural fates. Nature 498:456–462. doi:10.1038/nature12319

Malin J, Desplan C. 2021. Neural specification, targeting, and circuit formation during visual system assembly. Proc Natl Acad Sci 118:e2101823118. doi:10.1073/pnas.2101823118

Maurange C, Cheng L, Gould AP. 2008. Temporal Transcription Factors and Their Targets Schedule the End of Neural Proliferation in Drosophila. Cell 133:891–902. doi:10.1016/j.cell.2008.03.034

McConnell SK, Kaznowski CE. 1991. Cell Cycle Dependence of Laminar Determination in Developing Neocortex. Science 254:282–285. doi:10.1126/science.1925583

Oberst P, Agirman G, Jabaudon D. 2019. Principles of progenitor temporal patterning in the developing invertebrate and vertebrate nervous system. Curr Opin Neurobiol 56:185–193. doi:10.1016/j.conb.2019.03.004

Ohnuma S, Harris WA. 2003. Neurogenesis and the Cell Cycle. Neuron 40:199–208. doi:10.1016/S0896-6273(03)00632-9

Ohtsuka T, Kageyama R. 2019. Regulation of temporal properties of neural stem cells and transition timing of neurogenesis and gliogenesis during mammalian neocortical development. Semin Cell Dev Biol 95:4–11. doi:10.1016/j.semcdb.2019.01.007

Okamoto M, Miyata T, Konno D, Ueda HR, Kasukawa T, Hashimoto M, Matsuzaki F, Kawaguchi A. 2016. Cell-cycle-independent transitions in temporal identity of mammalian neural progenitor cells. Nat Commun 7:11349. doi:10.1038/ncomms11349

Pebworth M-P, Ross J, Andrews M, Bhaduri A, Kriegstein AR. 2021. Human intermediate progenitor diversity during cortical development. Proc Natl Acad Sci 118:e2019415118. doi:10.1073/pnas.2019415118

Pahl MC, Doyle SE, Siegrist SE. 2019. E93 Integrates Neuroblast Intrinsic State with Developmental Time to Terminate MB Neurogenesis via Autophagy. Curr Biol 29:750-762.e3. doi:10.1016/j.cub.2019.01.039

Ray A, Li X. 2022. A Notch-dependent transcriptional mechanism controls expression of temporal patterning factors in Drosophila medulla. eLife 11:e75879. doi:10.7554/eLife.75879

Ren Q, Awasaki T, Wang Y-C, Huang Y-F, Lee T. 2018. Lineage-guided Notch-dependent gliogenesis by Drosophila multi-potent progenitors. Development dev.160127. doi:10.1242/dev.160127

Ren Q, Yang C-P, Liu Z, Sugino K, Mok K, He Y, Ito M, Nern A, Otsuna H, Lee T. 2017. Stem Cell-Intrinsic, Seven-up-Triggered Temporal Factor Gradients Diversify Intermediate Neural Progenitors. Curr Biol 27:1303–1313. doi:10.1016/j.cub.2017.03.047

Rossi AM, Desplan C. 2017. Asymmetric Notch Amplification to Secure Stem Cell Identity. Dev Cell 40:513–514. doi:10.1016/j.devcel.2017.03.010

Salomoni P, Calegari F. 2010. Cell cycle control of mammalian neural stem cells: putting a speed limit on G1. Trends Cell Biol 20:233–243. doi:10.1016/j.tcb.2010.01.006

Sen SQ. 2023. Generating neural diversity through spatial and temporal patterning. Semin Cell Dev Biol 142:54–66. doi:10.1016/j.semcdb.2022.06.002

Skeath JB, Thor S. 2003. Genetic control of Drosophila nerve cord development. Curr Opin Neurobiol 13:8–15. doi:10.1016/S0959-4388(03)00007-2

Sood C, Nahid MA, Branham KR, Pahl M, Doyle SE, Siegrist SE. 2024. Delta-dependent Notch activation closes the early neuroblast temporal program to promote lineage progression and neurogenesis termination in Drosophila. eLife 12:RP88565. doi:10.7554/eLife.88565.3

Syed MH, Mark B, Doe CQ. 2017. Steroid hormone induction of temporal gene expression in Drosophila brain neuroblasts generates neuronal and glial diversity. eLife 6:e26287. doi:10.7554/eLife.26287

Telley L, Agirman G, Prados J, Amberg N, Fièvre S, Oberst P, Bartolini G, Vitali I, Cadilhac C, Hippenmeyer S, Nguyen L, Dayer A, Jabaudon D. 2019. Temporal patterning of apical progenitors and their daughter neurons in the developing neocortex. Science 364:eaav2522. doi:10.1126/science.aav2522

van den Ameele J, Brand AH. 2019. Neural stem cell temporal patterning and brain tumour growth rely on oxidative phosphorylation. eLife 8:e47887. doi:10.7554/eLife.47887

Walsh KT, Doe CQ. 2017. Drosophila embryonic type II neuroblasts: origin, temporal patterning, and contribution to the adult central complex. Development dev.157826. doi:10.1242/dev.157826

Wang Y-C, Yang JS, Johnston R, Ren Q, Lee Y-J, Luan H, Brody T, Odenwald WF, Lee T. 2014. Drosophila intermediate neural progenitors produce lineage-dependent related series of diverse neurons. Development 141:253–258. doi:10.1242/dev.103069

Wani AR, Chowdhury B, Luong J, Chaya GM, Patel K, Isaacman-Beck J, Shafer O, Kayser MS, Syed MH. 2023. Stem cell-specific ecdysone signaling regulates the development and function of a Drosophila sleep homeostat (preprint). Neuroscience. doi:10.1101/2023.09.29.560022

Yang C-P, Fu C-C, Sugino K, Liu Z, Ren Q, Liu L-Y, Yao X, Lee LP, Lee T. 2015. Transcriptomes of lineage-specific Drosophila neuroblasts profiled via genetic targeting and robotic sorting. Development dev.129163. doi:10.1242/dev.129163

Resource Table

Antibodies	**Source**	**Identifier**
Chicken anti-GFP (1:å1500)	Aves Labs	Cat# AB_2314866; RRID_AB_2314866
Rabbit anti-Asense (1:1000)	Chien-Yu Lee	N/A
Rat anti-IMP (1:200)	Claude Desplan	N/A
Rabbit anti b -GAL (1:1000)	MP Biomedicals	Cat# 559762
Mouse anti-EcR-B1 (1:2000)	Carl Thummel	N/A
Guinea pig anti-Syncrip (1:2000)	Ilan Davis	N/A
Chemicals		
16% Paraformaldehyde	Electron Microscopy Sciences	Cat# 15710
Triton X-100	Sigma-Aldrich	Cat# T8787
Apple Juice	S. Martinelli & Co	N/A
Schneider's Insect medium	Sigma-Aldrich	Cat# S0146
Agar	Sigma-Aldrich	Cat# A1296
DPX mounting medium	Sigma-Aldrich	Cat# 06522
Sucrose	Research products International	Cat# 57-50-1
Xylene	Fisher Scientific	Cat# 1330-20-7, 100-41-4

Strains		
hsFlp,UAS-mCD8GFP; Act-FRTstopFRT-GAL4	This study	NA
UAS-pavRNAi	BDSC	BDSC_43963
UAS-Cdk1RNAi	BDSC	BDSC_36117
UAS-mCherryRNAi	BDSC	BDSC_35785
Wor-GAL4, Ase-GAL80; 20xUASmcd8GFP	Syed Lab	NA
Wor-GAL4, Ase-GAL80; tub-GAL80ts	Syed Lab	NA
UAS-mcd8GFP (II)	BDSC	5137
20xUAS-mcd8GFP (III)	BDSC	32194
svp-LacZ	BDSC	BDSC_26669
Software and Algorthms		
Imagej	Fiji	Version: 2.9.0/1.53t
Adobe Illustrator (version 24.005.20307)	Adobe Systems	
GraphPad Prism 9	GraphPad Software	https://www.graphpad.com/
Imaris v9.9 and above	Oxford Instruments	RRID: SCR_007370; https://www.oxinst.com/news/imaris-launches-version-9.9-with-machine-learning-and-open-source-connections

Fly Genotype with Associated Figures

Experimental line	**Main**	**Supplementary**
hsFlp,UAS-GFP;Act-FRTstopFRT-GAL4 crossed to UAS-mCherryRNAi	Fig. 2A, 2B, 2C	Fig. S1A
hsFlp,UAS-GFP; Act-FRTstopFRT-GAL4 crossed to UAS-Cdk1RNAi	Fig. 2D, 2E, 2F,	Fig. S1B
hsFlp,UAS-GFP;act-FRTstopFRT-GAL4 crossed to UAS-pavRNAi	Fig. 2G, 2H, 2I	Fig. S1C
Wor-GAL4, Ase-GAL80;tub-GAL80ts crossed to UAS-mcd8::GFP;UAS-mCherryRNAi		Fig. S2A-A’’’

Wor-GAL4, Ase-GAL80;tub-GAL80ts crossed to UAS-mcd8::GFP;UAS-Cdk1RNAi		Fig. S2B-B’’’
Wor-GAL4, Ase-GAL80;tub-GAL80ts crossed to UAS-mcd8::GFP;UAS-pavRNAi		Fig. S2C-C’’’
Wor-GAL4,AseGAL80; 20xUASmcd8:GFP crossed to Svp-LacZ	Fig. 3A	
WorGAL4,AseGAL80; 20xUASmcd8:GFP crossed to UAS-Cdk1-RNAi;Svp-LacZ	Fig. 3B	
hsFlp,UASmCD8GFP; Act-FRTstopFRT-GAL4 crossed to UAS-mCherryRNAi	Fig. 4A, 4B, 4C	
hsFlp,UASmCD8GFP; Act-FRTstopFRT-GAL4 crossed to UAS-Cdk1RNAi	Fig. 4D, 4E, 4F	
hsFlp,UASGFP; Act-FRTstopFRT-GAL4 crossed to UAS-pavRNAi	Fig. 4G, 4H, 4I	
hsFlp,UASmCD8GFP; Act-FRTstopFRT-GAL4 crossed to UAS-mCherryRNAi	Fig. 5A, 5B, 5C, 5K, 5L, 5M	
hsFlp,UASmCD8 GFP; Act-FRTstopFRT-GAL4 crossed to UAS-Cdk1RNAi	Fig. 5D, 5E, 5F, 5N, 5O, 5P	
hsFlp,UASGFP; Act-FRTstopFRT-GAL4 crossed to UAS-pavRNAi	Fig. 5G, 5H, 5I, 5Q, 5R, 5S	

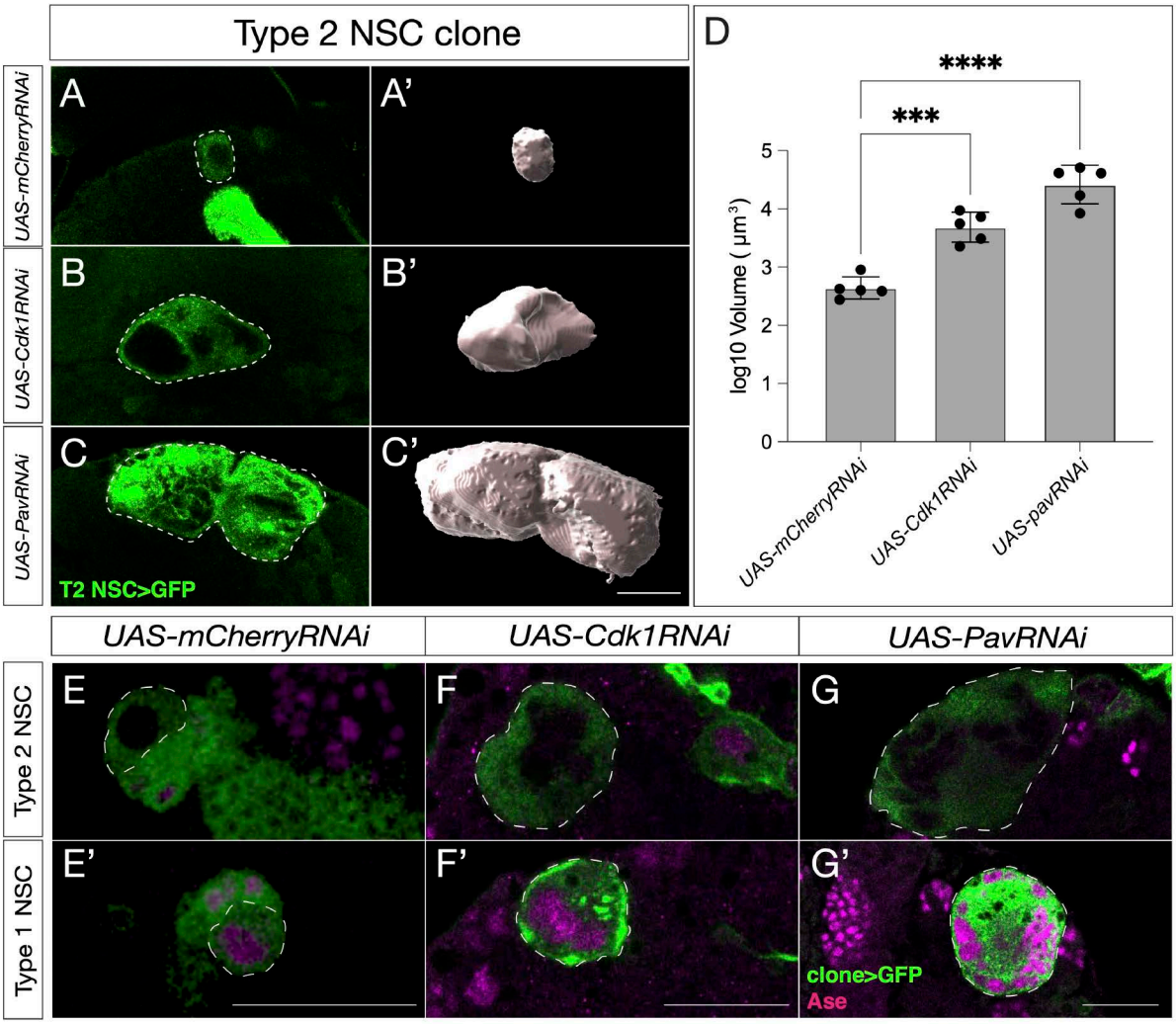

Figure S1: pav and Cdk1RNAi type 2 NSC clones are larger in volume. Confocal scans with their respective Imaris reconstruction are shown on the right for mCherryRNAi (A-A'), Cdk1RNAi (B-B'), and pavRNAi (C-C') clones. (D) Quantification of log10-transformed clone volumes (µm^3); n = 5 clones per condition, plotted as mean ± SEM. Overall treatment effect by Welch's ANOVA, $p < 0.0001$. Post-hoc Dunnett's T3 vs. mCherryRNAi: Cdk1RNAi, $p = 0.0003$; pavRNAi, $p < 0.0001$. only one clone was quantified per animal. Type 2 (E–G) and type 1 (E'–G') clones show negative and positive nuclear Asense (Ase) staining, respectively, in (E, E') mCherryRNAi, (F, F') Cdk1RNAi, and (G, G') pavRNAi. Scale bar represents 20um.

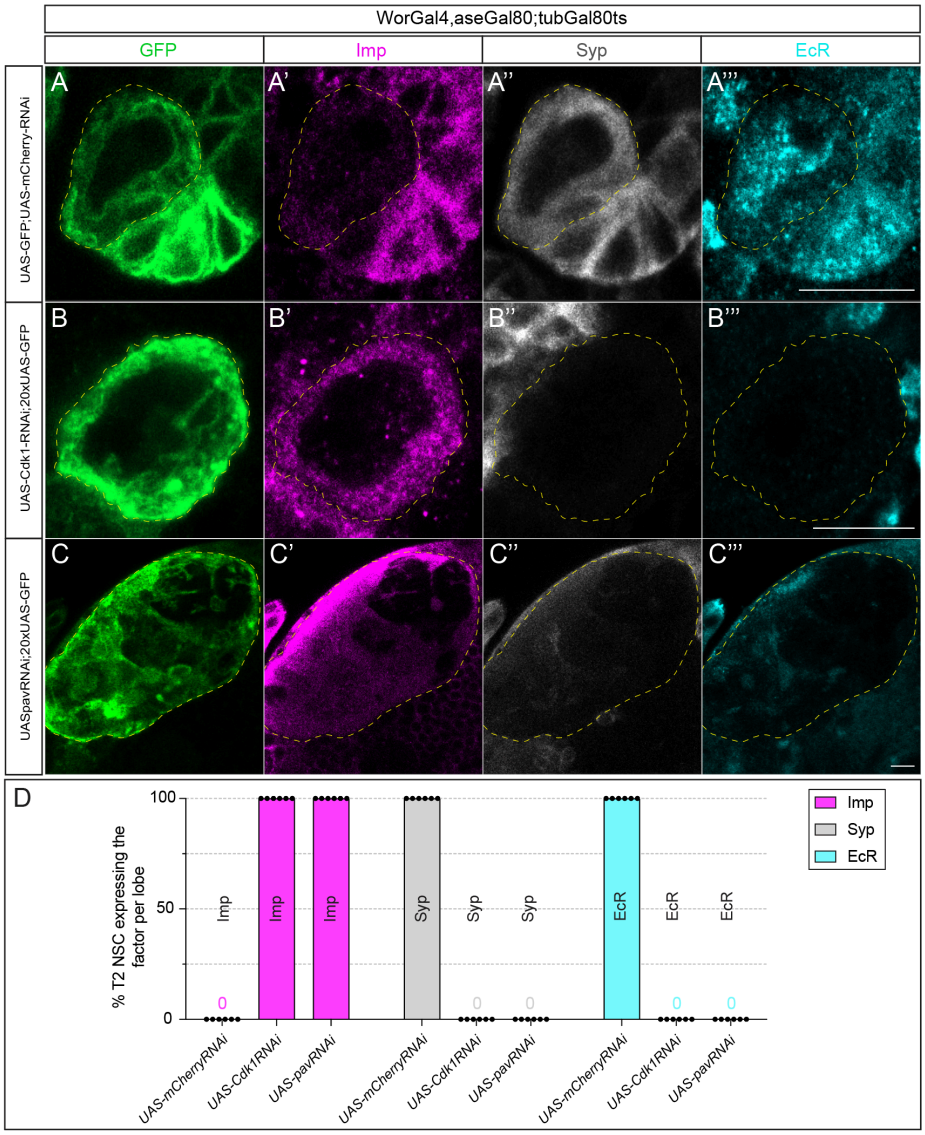

Figure S2: Cell-cycle and cytokinesis inhibit the early-to-late transition of temporal factors in type 2 NSCs. (A-A''') Type 2 NSC control UAS-mCherryRNAi (circled) at 72h ALH show normal temporal gene expression progression. Early factor Imp is off, and late factors Syp and EcR are on at 72h ALH (B-B''''). Cdk1RNAi type 2 NSCs fail to downregulate early factor Imp, and late factors Syp and EcR are not turned on. (C-C''') Similarly, cytokinesis-blocked type 2 NSCs using pavRNAi fail to downregulate Imp and upregulate Syp and EcR. (D) Quantifications of early and late temporal factor expression in control, cell cycle, and cytokinesis blocked type 2 NSCs; n=6 for each genotype. Type 2 NSCs are identified as large cells expressing UAS-mcd8::GFP. Scale bars represent 10um.